Linear Quadratic Integral Differential Game applied to the Real-time Control of a Quadrotor Experimental setup

Hadi Nobahari*, Alireza Sharifi

Sharif University of Technology, Zip Code 1458889694, Tehran, Iran
nobahari@sharif.edu, alireza_sharifi@ae.sharif.edu

Abstract.

The accurate attitude control of a quadrotor is necessary, especially when facing disturbance. In this study, a linear quadratic with integral action based on the differential game theory is implemented on a quadrotor experimental setup. A continuous state-space model of the setup is derived using the linearization of nonlinear equations of motion, and its parameters are identified with the experimental results. Then, the attitude control commands of the quadrotor are derived based on two players; one finds the best attitude control command, and the other creates the disturbance by mini-maximizing a quadratic criterion, defined as the sum of outputs plus the weighted control effort and disturbance. The performance of the proposed structure is investigated in level flight and compared to the linear quadratic regulator controller. Results demonstrate that the proposed approach has an excellent performance in dissipating the disturbances. (Ali)

Keywords: Linear Quadratic Differential Game, Quadrotor, Real-time, 3DoF Experimental setup, Optimal Control, Robust Control.

*Corresponding Author.

1 Introduction

A quadrotor is a type of helicopter with four rotors that plays a significant role in today's society, including research, military, imaging, recreation, and agriculture. The performance of the quadrotor relies on the control system, including attitude, altitude, and position subsystems. In the attitude control of the quadrotor, it is vital to maintain the attitude outputs at the desired level using control commands such as the rotational speed of the rotors, when the disturbances occur suddenly. Therefore, much research is being conducted on the automatic control of the attitudes' quadrotor in facing the disturbance.

In \cite{PID}, a Proportional Integral Derivative (PID) controller is used to regulate the quadrotor attitude. However, the control objectives have not been effectively achieved with this controllers when the disturbance occurs. To solve this problem the model-based approaches \cite{model_base} are utilized for controller design. These controllers work based on information from the quadrotor's attitude model and disturbance to produce the best control command.

Various model-based controllers can be found within the literature, the most well-known of which are intelligent control, the nonlinear control, robust control, and optimal control to reduce the disturbance effect in the attitude control and provide a faster control algorithm in facing the modeling error. In the intelligent controller category, the artificial intelligence computing approaches like fuzzy logic \cite{fuzzy}, iterative learning \cite{iterative_Learning}, machine learning \cite{machine_learning}, reinforcement learning \cite{Reinforcement_Learning}, and evolutionary computation \cite{Evolutionary} have been utilized to regulate the quadrotor's attitude.

Moreover, nonlinear control methods such as Feedback Linearization (FBL) \cite{FBL} and Sliding Mode Control (SMC) \cite{SMC} have been applied to control the roll, pitch, and yaw angles of the quadrotor. In the optimal controller category, a Linear Quadratic

Regulator (LQR) \cite{LQR} and Linear Quadratic Gaussian (LQG) \cite{LQG} have been implemented on the quadrotor based on the minimization of a quadratic criterion, including regulation performance and control effort to provide optimally controlled feedback gains.

Linear Quadratic Regulator Differential Game (LQR-DG) control approach \cite{LQDG, robust_LQDG} is a class of optimal and robust controller methods that controls the outputs of a system based on its linear model and mini-maximization of a cost function. This approach has been utilized to stabilize and control various nonlinear and complex systems such as a ship controller \cite{LQDG_ship}. Moreover, in the LQR-DG control method, the control commands are analytically generated based on a pursuit-evasion of two players, one tracks the best control command, and the other creates the disturbance. This is one of the distinctive features of the LQR-DG controller and an important difference from other optimal control methods.

In this study, an LQR controller method based on the differential game theory, with an integral action called Linear Quadratic Integral Regulator Differential Game (LQIR-DG) controller, is proposed to generate the most efficient control command for an experimental setup of the quadrotor when facing the disturbance. Since the LQIR-DG is affected by an accurate model of the system, first, the dynamic of the three-degree-of-freedom setup of the quadrotor is modeled. Then, the linear state-space form the quadrotor model is extracted using the linearization of the nonlinear equations of motion to utilize in the proposed control problem. Moreover, the model's parameters are identified and verified against the experimental values. Next, the LQIR-DG technique is applied to the experimental setup of the quadrotor to reduce the effect of disturbance. The performance of the suggested controller is examined when the disturbance occurs. The results show the successful performance of the LQIR-DG scheme in reducing the disturbance.

In the remainder of this study, the problem is defined in section \ref{sec:problem_statement}. The dynamics model for the experimental setup of the quadrotor is derived in details, in section \ref{sec:modeling}. In section \ref{sec: diff game}, The LQIR-DG architecture is denoted. Finally, in sections \ref{sec:results} and \ref{sec:conclusion}, Numerical results and conclusion are provided, respectively.

2 Problem Statement

Here, the model of the three-degree-of-freedom setup of the quadrotor is presented in details. Here, a nonlinear dynamic is presented for the setup of the quadrotor, as illustrated in \figurename{\ref{quadlab}}. The quadrotor is free to rotate about its roll, pitch, and yaw axes. The Euler angles and angular velocities along three orthogonal axes are measured simultaneously using the Attitude and Heading Reference Systems (AHRS). These noisy measurements are utilizes in the LQIR-DG for control of the Euler angles. The block diagram of the controller structure is illustrated in \figurename{\ref{block_diagram}}.

Fig. 1. 3DoF setup of the quadrotor

3 Modeling of the Quadrotor Setup

Here, the model of the three-degree-of-freedom setup of the quadrotor is presented in details. For this purpose, first, the configuration of the quadrotor is denoted. Then, the nonlinear model of the attitude dynamics is derived to denote the state-space form. Finally, the nonlinear model is linearized to utilize in the control purposes.

3.1 Configuration of the Quadrotor

\figurename{\ref{QuadAssum}} denotes the quadrotor schematic. Each rotor has an angular velocity, Ω_i, rotating about the z_B axis in the body coordinate system. Rotors 1 and 3 rotate counterclockwise, while rotors 2 and 4 rotate clockwise, to cancel yawing moment.

3.2 Dynamic Model

The quadrotor kinetic model, derived using the Newton-Euler method, is stated as \cite{b15}, \cite{b16}

$$\dot{p} = \frac{\mathrm{I}_{yy} - \mathrm{I}_{zz}}{\mathrm{I}_{xx}} qr + q \frac{\mathrm{I}_{rotor}}{\mathrm{I}_{xx}} \Omega_r + \frac{u_{roll}}{\mathrm{I}_{xx}} + \frac{d_{roll}}{\mathrm{I}_{xx}}$$

$$\dot{q} = \frac{\mathrm{I}_{zz} - \mathrm{I}_{zz}}{\mathrm{I}_{yy}} rp + p \frac{\mathrm{I}_{rotor}}{\mathrm{I}_{xx}} \Omega_r + \frac{u_{pitch}}{\mathrm{I}_{yy}} + \frac{d_{pitch}}{\mathrm{I}_{yy}}$$

$$\dot{r} = \frac{\mathrm{I}_{xx} - \mathrm{I}_{yy}}{\mathrm{I}_{zz}} pq + \frac{u_{yaw}}{\mathrm{I}_{zz}} + \frac{d_{yaw}}{\mathrm{I}_{zz}}$$

where (p,q,r) are the angular velocities. d_{roll}, d_{pitch}, and d_{yaw} are the disturbances, generated in x_B, y_B. and z_B, respectively. Moreover, I_{xx}, I_{yy}, and I_{zz} are the principal moment of inertia and I_{rotor} is a rotor inertia about its axis. The relation between the angular body rates and the Euler angles rates are obtained as

$$\dot{\phi} = p + (q\sin(\phi) + r\cos(\phi))\tan(\theta)$$ **Error! Reference source not found.**

$$\dot{\theta} = q\cos(\phi) - r\sin(\phi)$$

$$\dot{\psi} = (q\sin(\phi) + r\cos(\phi))/\cos(\theta)$$

where (ϕ, θ, ψ) are roll, pitch, and yaw angles. Moreover, Ω_r, called the overall residual rotor angular velocity, is computed as

$$\Omega_r = -\Omega_1 + \Omega_2 - \Omega_3 + \Omega_4$$

3.3 Control Commands

The control inputs u_{roll}, u_{pitch}, and u_{yaw} are roll, pitch, and yaw moments, obtained from the rotors, defined as

$$u_{\text{roll}} = \text{bd}_{\text{cg}}(\Omega_2^2 - \Omega_4^2)$$

$$u_{\text{pitch}} = \text{bd}_{\text{cg}}(\Omega_1^2 - \Omega_3^2)$$

$$u_{\text{yaw}} = \text{d}(\Omega_1^2 - \Omega_2^2 + \Omega_3^2 - \Omega_4^2)$$

Also, d and b are, respectively, drag and thrust coefficients. d_{cg} is the distance of rotors from the gravity center . Hence, the angular velocity commands are obtained as

$$\Omega_{c,1}^2 = \Omega_{\text{mean}}^2 + \frac{1}{2\text{bd}_{\text{cg}}}u_{\text{pitch}} + \frac{1}{4d}u_{\text{yaw}}$$

$$\Omega_{c,2}^2 = \Omega_{\text{mean}}^2 + \frac{1}{2\text{bd}_{\text{cg}}}u_{\text{roll}} - \frac{1}{4d}u_{\text{yaw}}$$

$$\Omega_{c,3}^2 = \Omega_{\text{mean}}^2 - \frac{1}{2\text{bd}_{\text{cg}}}u_{\text{pitch}} + \frac{1}{4d}u_{\text{yaw}}$$

$$\Omega_{c,4}^2 = \Omega_{\text{mean}}^2 - \frac{1}{2\text{bd}_{\text{cg}}}u_{\text{roll}} - \frac{1}{4d}u_{\text{yaw}}$$

where Ω_{mean} is the nominal of the rotor angular velocities.

3.4 State-Space Form

Here, the state-space model is presented for the control purposes. By defining $x_1 = p$, $x_2 = q$, $x_3 = r$, $x_4 = \phi$, $x_5 = \theta$, and $x_6 = \psi$; the model of in state-space form are denoted as

$$\dot{x_1} = \frac{\mathrm{I_{yy}} - \mathrm{I_{zz}}}{\mathrm{I_{xx}}} x_2 x_3 + x_2 \frac{\mathrm{I_{rotor}}}{\mathrm{I_{xx}}} \Omega_r + \frac{u_{\mathrm{roll}}}{\mathrm{I_{xx}}} + \frac{d_{\mathrm{roll}}}{\mathrm{I_{xx}}}$$

$$\dot{x_2} = \frac{\mathrm{I_{zz}} - \mathrm{I_{zz}}}{\mathrm{I_{yy}}} x_1 x_3 - x_1 \frac{\mathrm{I_{rotor}}}{\mathrm{I_{xx}}} \Omega_r + \frac{u_{\mathrm{pitch}}}{\mathrm{I_{yy}}} + \frac{d_{\mathrm{pitch}}}{\mathrm{I_{yy}}}$$

$$\dot{x_3} = \frac{\mathrm{I_{xx}} - \mathrm{I_{yy}}}{\mathrm{I_{zz}}} x_1 x_2 + \frac{u_{\mathrm{yaw}}}{\mathrm{I_{zz}}} + \frac{d_{\mathrm{yaw}}}{\mathrm{I_{zz}}}$$

$$\dot{x_4} = x_1 + (x_2 \sin(x_4) + x_3 \cos(x_4)) \tan(x_5)$$

$$\dot{x_5} = x_2 \cos(x_4) - x_3 \sin(x_4)$$

$$\dot{x_6} = (x_2 \sin(x_4) + x_3 \cos(x_4)) / \cos(x_5)$$

The measurement model is written as

$$\mathrm{z} = \begin{bmatrix} p_m & q_m & r_m & \phi_m & \theta_m & \psi_m \end{bmatrix}^{\mathrm{T}}$$

3.5 Linear Model

The continuous-time linear model is utilized to drive the control commands on the quadrotor. The linear state-space model is denoted as

$$\dot{\mathrm{x}}(t) = \mathrm{A}\mathrm{x}(t) + \mathrm{B}\mathrm{u}(t) + \mathrm{B_d}\mathrm{d}(t)$$

where A, B, and $\mathrm{B_d}$ are the system, input and disturbance matrices, respectively. Moreover, d is the disturbance. The measurements equation is stated as

$$\mathrm{z}(t) = \mathrm{x}(t)$$

According to Eqs.\eqref{eq:diffeq}-\eqref{eq:diffeq-end}, the linear dynamic model around the equilibrium points $(\mathrm{x}_e = 0 \text{ and } \mathrm{u}_e = 0)$ of. the quadrotor setup is denoted as

$$\boldsymbol{\mathrm{\dot{x}}} = \begin{bmatrix} \boldsymbol{\mathrm{\dot{x}}_{\text{roll}}} \\ \boldsymbol{\mathrm{\dot{x}}_{\text{pitch}}} \\ \boldsymbol{\mathrm{\dot{x}}_{\text{yaw}}} \end{bmatrix} = \begin{bmatrix} \boldsymbol{\mathrm{A}_{\text{roll}}} & \boldsymbol{0} & \boldsymbol{0} \\ \boldsymbol{0} & \boldsymbol{\mathrm{A}_{\text{pitch}}} & \boldsymbol{0} \\ \boldsymbol{0} & \boldsymbol{0} & \boldsymbol{\mathrm{A}_{\text{yaw}}} \end{bmatrix} \begin{bmatrix} \boldsymbol{\mathrm{x}_{\text{roll}}} \\ \boldsymbol{\mathrm{x}_{\text{pitch}}} \\ \boldsymbol{\mathrm{x}_{\text{yaw}}} \end{bmatrix} + \begin{bmatrix} \mathrm{B}_{\text{roll}} & \boldsymbol{0} & \boldsymbol{0} \\ \boldsymbol{0} & \mathrm{B}_{\text{pitch}} & \boldsymbol{0} \\ \boldsymbol{0} & \boldsymbol{0} & \mathrm{B}_{\text{yaw}} \end{bmatrix} \begin{bmatrix} \mathrm{u}_{\text{roll}} \\ \mathrm{u}_{\text{pitch}} \\ \mathrm{u}_{\text{yaw}} \end{bmatrix} + \begin{bmatrix} \mathrm{B}_{\text{roll}} & \boldsymbol{0} & \boldsymbol{0} \\ \boldsymbol{0} & \mathrm{B}_{\text{pitch}} & \boldsymbol{0} \\ \boldsymbol{0} & \boldsymbol{0} & \mathrm{B}_{\text{yaw}} \end{bmatrix} \begin{bmatrix} \mathrm{d}_{\text{roll}} \\ \mathrm{d}_{\text{pitch}} \\ \mathrm{d}_{\text{yaw}} \end{bmatrix}$$

where $\mathrm{x}_{\text{roll}} = \begin{bmatrix} p & \phi \end{bmatrix}^{\mathrm{T}}$, $\mathrm{x}_{\text{pitch}} = \begin{bmatrix} q & \theta \end{bmatrix}^{\mathrm{T}}$, and $\mathrm{x}_{\text{yaw}} = \begin{bmatrix} r & \psi \end{bmatrix}^{\mathrm{T}}$.

Moreover, the state and input matrices are presented as

$$A_{roll} = A_{pitch} = A_{yaw} = \begin{bmatrix} 0 & 0 \\ 1 & 0 \end{bmatrix}$$

$$B_{roll} = \begin{bmatrix} \frac{1}{I_{xx}} \\ 0 \end{bmatrix}. B_{pitch} = \begin{bmatrix} \frac{1}{I_{yy}} \\ 0 \end{bmatrix}; B_{yaw} = \begin{bmatrix} \frac{1}{I_{zz}} \\ 0 \end{bmatrix}$$

4 Formulation of the Controller Design

In the LQIR-DG controller structure, an integral action is added to the LQR-DG controller to cancel the steady-state errors for reference tracking. For this purpose, first, the augmented state space of the linear quadrotor model is defined to utilize in the controller architecture. Then, the LQR-DG controller design procedure is presented to produce the best control commands for the experimental setup of the quadrotor.

4.1 Augmented State Space Formulation

To add the integral action to the controller structure, the augmented states are defined as follows:

$$x_{a_i} = \begin{bmatrix} x_i & \int x_i \end{bmatrix}^T$$

.where i = roll, pitch, and yaw.

Then, the quadrotor dynamics model, denoted by Eq.\eqref{eq:linear}, is denoted in the augmented state-space model as

$$\dot{x}_a(t) = A_a x_a(t) + B_a u(t) + B_{d_a} d(t)$$

where matrices A_a and B_a are defined as follows:

$$A_a = \begin{bmatrix} A & \mathbf{0} \\ I & \mathbf{0} \end{bmatrix}$$

$$B_a = B_{d_a} = \begin{bmatrix} B \\ \mathbf{0} \end{bmatrix}$$

In the above equation I denotes the identity matrix.

4.2 LQIR-DG Controller Method

The LQIR-DG controller is an optimal and robust method based on the differential game theory. This controller consists of two essential players: one finds the best control command, and the other creates the worst disturbance.

For this purpose, the first player tries to minimize a cost function; while the second player is assumed to maximize it. Therefore, the quadratic cost function equation is denoted using min-max operators as follows:

$$\min_u \max_d J(x_{a_i}, u_i, d_i) = J(x_{a_i}, u_i^*, d_i^*) = \min_u \max_d \int_0^{t_f} \left(x_{a_i}^T Q_i x_{a_i} + u_i^T R u_i - d_i^T R_d d_i \right) dt$$

where ${{ R}}$ and ${{R_{d}}}$ are symmetric nonnegative definite matrices and $\boldsymbol{\mathrm{Q_i}} $ is a symmetric positive definite matrix. Moreover, $\mathrm{t_f}$ is the final time. To solve this problem, connections between the general optimal problem and the LQIR problem are considered \cite{LQDG} and consequently the optimum control effort is computed for the each control loop as follows:

$$u_i(t) = -K_i(t) x_{a_i}(t)$$

$$d_i(t) = K_i(t) x_{a_i}(t)$$

where K_i and K_{d_i} are a time varying gain, given by

$$K_i = R^{-1} B_{a_i}^T P_{a_i}(t)$$

$$K_{d_i} = R_d^{-1} B_{\mathbf{a_{d_i}}}^{T} P_{\mathbf{a_{d_i}}}(t)$$

where $P_{\mathbf{a_i}}(t)$ and $P_{\mathbf{a_{d_i}}}(t)$ satisfy

$$\dot{P}_{\mathbf{a_i}}(t) = -A_a^{T} P_{a_i}(t) - P_{a_i}(t) A_a - Q_i + P_{a_i}(t) S_{a_i}(t) P_{a_i}(t) + P_{a_i}(t) S_{a_{d_i}}(t) P_{a_{d_i}}(t) \quad \text{(Ali)}$$

$$\dot{P}_{\mathbf{a_{d_i}}} \&(t) = -A_a^{T} P_{a_{d_i}}(t) - P_{a_{d_i}}(t) A_a - Q_i + P_{a_{d_i}}(t) S_{a_{d_i}}(t) P_{a_{d_i}}(t) + P_{a_{d_i}}(t) S_{a_i}(t) P_{a_i}(t)$$

where $S_{a_i} = B_{a_i} R^{-1} B_{\mathbf{a_i}}^{T}$ and $S_{a_{d_i}} = B_{\mathbf{a_{d_i}}} R_d^{-1} B_{\mathbf{a_{d_i}}}^{T}$.

In this study, the steady-state values of the above equations $(P \text{ as } t_f \to \infty)$ are utilized to generate a feedback control law.

5 Result and Discussion

Here, the results of the LQIR-DG controller method are devoted to the control loops of the roll, pitch, and yaw of the experimental setup of the quadrotor. First, the controller parameters are tuned using the results of numerical simulations. Moreover, the performance of the LQIR-DG controller is compared to an LQR control strategy. The quadrotor parameters are shown in table \ref{tab:parameters}.

Table 1. The Parameter of the Quadrotor.

Parameter	Unit	Value
Roll	Q_{roll}	diag([7.91, 0.01, 631.85, 214.28])
Pitch	Q_{pitch} .	
Yaw	Q_{yaw}	
-	R	diag([9853.09, 0.12, 0.01, 873.93])$diag$([1.81e\!-\!4$, $4.5e-4$, $3e-6$, $1.7e-5$])
0	R_d	1 $ 1.2577$

Table 2. The Parameters of the LQIR-DG Controller.

Control Loop	Weight	Value
I_{xx}	$kg.m^2$	\$0.02839\$
I_{yy}	$kg.m^2$	\$0.03066\$
I_{zz}	$kg.m^2$	\$0.0439\$
I_{rotor}	$kg.m^2$	4.4398×10^{-5}
b	$N.sec^2/rad^2$	3.13×10^{-5}
d	$N.m.sec^2/rad^2$	3.2×10^{-6}
Ω_{mean}	rpm	\$3000\$
d_{cg}	m	\$0.2\$

5.1 Performance of the LQIR-DG Controller

Here, the performance of the LQIR-DG controller is evaluated. The desired and actual outputs, including the roll, pitch, and yaw angles, are compared in \figurename{\ref{fig:result}}. The desired scenario of the simulator is considered as a level flight. These figures show that the attitude outputs of the quadrotor converge to the desired values in less than three seconds. Moreover, \figurename{\ref{fig:omega}} show the angular velocity command of the quadrotor,

respectively. These results illustrate that the LQIR-DG approach appropriately controls the attitude of the experimental setup of the quadrotor.

5.2 Comparison with LQR

Here, the LQIR-DG controller performance is compared with famous control strategy such as LQR controller method. \figurename{\ref{fig:compare}} compares the quadrotor's desired and actual pitch angle in the presence of these controllers. This results indicates that the LQIR-DG controller can provide high tracking performance, such as good transient response and high rapid convergence relative to LQR controller for pitch angle control of the quadrotor setup.

5.3 Comparison with LQR

\noindent Here, the LQIR-DG controller performance is compared with famous control strategy such as LQR controller method. \figurename{\ref{fig:compare}} compares the quadrotor's desired and actual pitch angle in the presence of these controllers. This results indicates that the LQIR-DG controller can provide high tracking performance, such as good transient response and high rapid convergence relative to LQR controller for pitch angle control of the quadrotor setup.

6 Conclusion

In this study, a linear quadratic with integral action based on the differential game theory, called LQIR-DG, was implemented for level attitude control in an experimental setup of a quadrotor. To implement the proposed controller structure, first, an accurate model of the quadrotor was linearized in the state-space form, and then the model parameters were estimated. Next, two players were considered for each of the quadrotor's roll, pitch, and yaw channels. The first player found the best control command for each channel of the setup of a quadrotor based on the mini-maximization of a quadratic criterion; when the second player produced the worst disturbances. Finally, the performance of the proposed controller was investigated in level

flight and compared to the LQR controller. The implementation results verify the successful performance of the LQIR-DG method in the level flight of the attitude control for the actual plant.

At the beginning of the inner loop, the priori position of the ants and the associated covariance are propagated. Next, the posteriori position of the ants is computed using EKF to estimate the current output. The estimated outputs are compared with the real measurement and each ant is assigned a cost, based on the quality of its estimation. Ants use their experience to update the pheromone distribution over the continuous state space. As in CACF **Error! Reference source not found.**, a normal function is utilized to model the pheromone distribution. Ants use this pheromone distribution to move from their current position toward the minimum cost estimation. The normal distribution permits all points of the state space to be chosen, either close to or far from the best point. The inner loop is terminated after a predefined number of iterations. Finally, the current state is estimated using a mean operator. In the following, these steps are discussed in detail.

Table 3. The parameters of the ECACF.

Parameter	Value	Description
N	10	Number of ants
i_{max}	5	Maximum number of iterations per step time
N_t	40%	Percent of top ants

Table 4. The noise model of the benchmark problems.

Experiment Number	Process noise			Measurement noise		
	Distribution	Parameter	Value	Distribution	Parameter	Value
1 [10, 11]	Gamma	Shape	3	Gaussian	Mean	0
		Scale	2		Variance	1×10^{-5}
2 **Error! Reference sourc not found.**	Gaussian	Mean	0	Gamma	Shape	7
		Variance	1×10^{-5}		Scale	2

The mean and the variance of the Root Mean Square Error (RMSE), obtained for 500 random runs, are presented in Table 5. It can be observed that the ECACF produces comparable and even better results than other filters in both cases. In addition, the variance of the ECACF is almost the smallest compared to other methods, implying that it has a stable performance according to **Error! Reference source not found.**. Moreover, the box plots and histograms, shown in Fig. 2, compare the RMSE of all filters. The cross line in each box plot indicates the median of the RMSE. The superiority of the ECACF is observed.

Table 5. Comparison of mean and variance of the RMSE obtained for 500 independent runs.

Filter	**RMSE for Experiment 1**		**RMSE for Experiment 2**	
	Mean	Variance	Mean	Variance
EPF	1.0326	1.0689	0.3463	0.0035
UPF	0.7525	0.4726	0.2816	0.0014
CACF	1.0861	0.0668	0.2813	0.0016
ECACF	0.3154	0.1142	0.2019	$1.107e^{-6}$

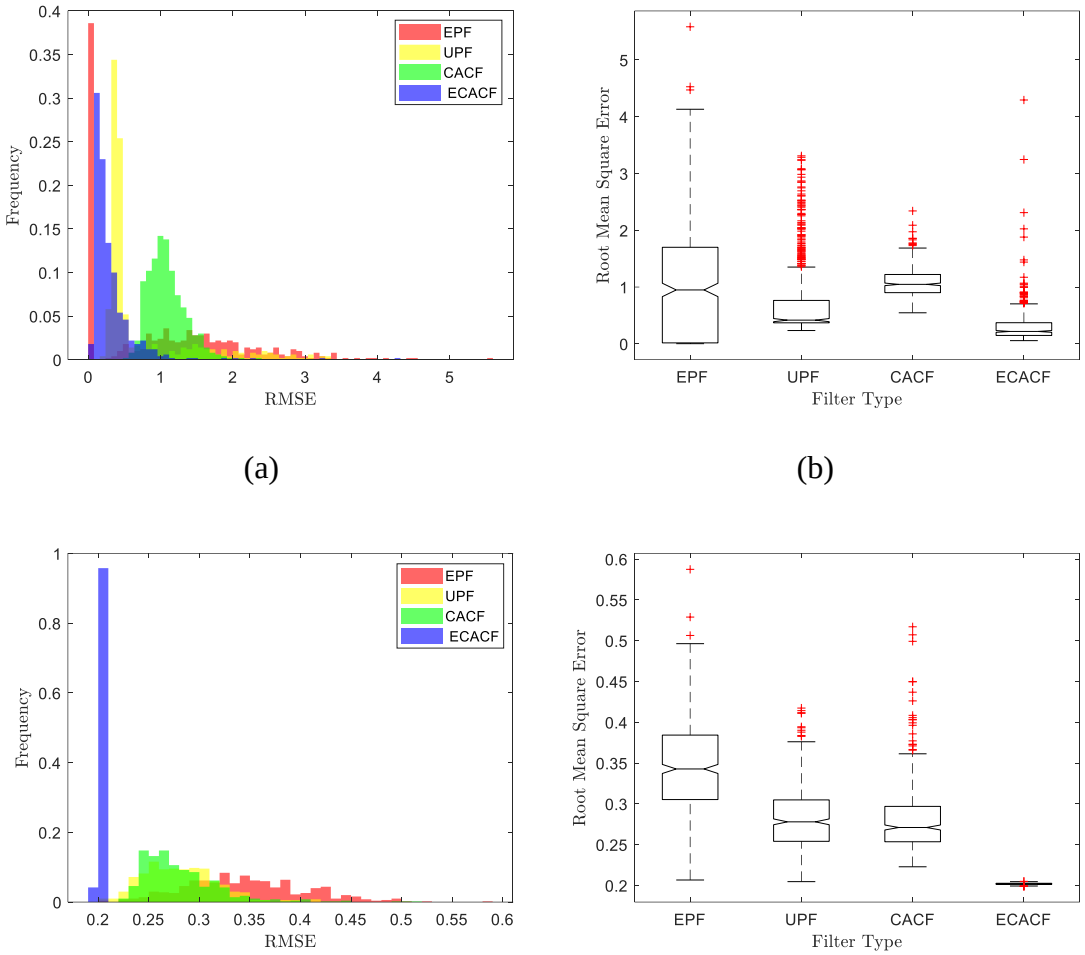

Fig. 2. Comparison of the RMSE obtained for 500 independent runs: (a) and (b) Experiment 1 (non-Gaussian process noise). (c) and (d) Experiment 2 (non-Gaussian measurement noise).

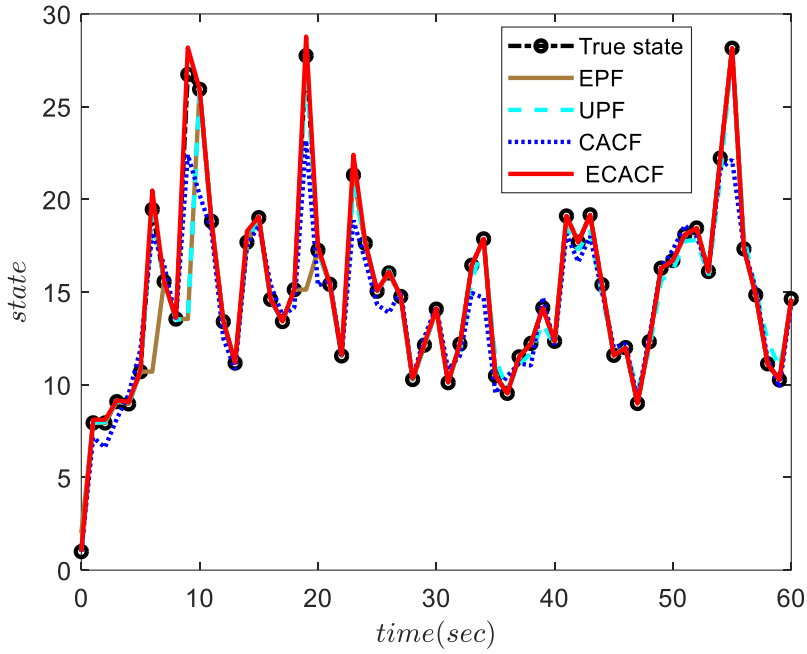

Table 6. Longitudinal Stability and Control Coefficients **Error! Reference source not found.**.

Parameter	Unit	Value
X_u	1/sec	-0.038
X_w	1/sec	-0.0513
X_q	ft/rad/sec	0.00152
X_e	ft/rad/sec^2	0.00005
X_t	ft/rad/sec^2	0.158
Z_u	1/sec	0.313
Z_w	1/sec	-0.605
Z_q	ft/rad/sec	-0.041
Z_e	ft/rad/sec^2	-0.146
Z_t	ft/rad/sec^2	0.031
M_u	rad/ft/sec	-0.0211
M_w	rad/ft/sec	0.157
M_q	1/sec	-0.612
M_e	1/sec^2	0.459
M_t	1/sec^2	0.0543